Isoform-Specific Divergent Roles of Class I HDACs in Cardiac Hypertrophic Remodeling

Mufeng Han

Beijing National Day School. Beijing China

mufenghan2007@outlook.com

Abstract. Class I histone deacetylases are emerging targets to manage cardiac hypertrophy. To delineate their individual roles, we used siRNA to knock down each HDAC isoform in human AC16 cardiomyocytes, in the presence or absence of angiotensin II (AngII). We found that HDAC1 and HDAC3 silencing could effectively reduce MYH7 expression and partially reverse cellular enlargement, whereas HDAC2 knockdown surprisingly exacerbated hypertrophy. Cross-isoform compensatory effects were also observed. RNA sequencing revealed distinct gene regulation profiles driven by different HDAC inhibitions. These results suggest that Class I HDAC isoforms mediate distinct, sometimes opposing, effects on cardiac hypertrophy.

Keywords: cardiac hypertrophy, Class I HDAC, knockdown, siRNA.

1. Introduction

Cardiovascular diseases remain the leading cause of global mortality. In China, they remain one of the greatest public health issues, accounting for over 40% of all deaths (National Center for Cardiovascular Diseases, The Writing Committee of the Report on Cardiovascular Health and Diseases in China, 2024). The pathological cardiac remodeling of such disease involves a critical cellular process: the hypertrophy of cardiomyocytes. This malignant process compromises cardiac structure and function, ultimately driving heart failure. Among the molecular drivers of such cellular pathologies, histone deacetylases (HDACs) are particularly relevant to the development of potential therapies.

HDACs play a critical role in chromatin remodeling and transcription regulation. By removing acetyl groups from lysine residues on histones and non-histone proteins, HDACs lead to chromatin compaction and transcriptional suppression, thereby influencing gene expression, DNA repair, and cell cycle progression (Gillette & Hill, 2015). HDACs are classified into four major groups based on structure and functional characteristics, including Class I, II, III, and IV. Within each class, multiple isoforms are present.

HDAC activity has been implicated in a variety of diseases, including cancer and cardiac conditions. In recent years, HDAC inhibitors (HDACi) have emerged as promising therapeutic agents (Kong et al., 2006). Initially developed to treat cancer by reversing the transcriptional silencing of tumor suppressor genes, HDACi are now being explored for their potential in reversing cardiac pathological remodeling. For example, pan-HDAC inhibitors have demonstrated efficacy in hypertensive mouse models by mitigating cardiac hypertrophy (Kee et al., 2006). Notably, the inhibition of Class I and II HDACs has shown opposing effects towards one another: while Class I HDAC inhibition provides cardioprotective benefits such as reduced hypertrophy, Class II HDAC inhibition has been associated with enhanced hypertrophic issues (Gillette, 2021). Within Class I, the suppression of HDAC1 and HDAC2 has been shown to inhibit mTOR signaling in neonatal rat cardiomyocytes (Morales et al., 2016).

Although existing studies have underscored the therapeutic potential of HDACi towards heart diseases such as cardiac hypertrophy, the specific roles and effects of inhibiting individual Class I HDAC isoforms (HDAC 1, 2, 3, or 8) remain poorly understood. Understanding which specific Class I HDAC isoforms drive cardiac pathological remodeling more significantly could provide valuable insights for the development of isoform-specific inhibitors. Such targeted approaches hold the promise of maximizing therapeutic efficacy while minimizing off-target effects, advancing the field

of cardiac disease treatment. This research seeks to address the research gap in the individual contributions of Class I HDAC isoforms to cardiac pathological remodeling.

2. Methods

2.1. Cell Culture

AC16 human cardiomyocyte cells were cultured in complete growth medium consisting of DMEM/F-12 (1:1) (Gibco, #11320033) supplemented with 10% fetal bovine serum (Gibco) at 37°C. Cells were passaged after reaching 80-90% confluency using a 0.25% trypsin-EDTA solution. For experiments, cells were seeded into 6-well culture plates and allowed to adhere for a minimum of 12 hours.

2.2. siRNA Knockdown

siRNAs were used to knock down Class I HDAC isoforms (Table 1) by transfection. Transfection was performed using the siRNA-mate plus transfection reagent (GenePharma) according to the manufacturer's protocol. AC16 cells were transfected with a non-targeting siRNA (negative control, NC) or with siRNA targeting HDAC1, 2, 3 at a range of concentrations (0.5x, 1.0x, 1.5x, and 2.0x the manufacturer's recommended concentration) using the siRNA-mate plus transfection reagent (Suzhou GenePharma Co., Ltd.). Cells were harvested 72 hours post-transfection and assessed via quantitative PCR and Western Blotting. A final concentration of 20 μM (1.0x recommended concentration) was selected for all subsequent experiments as it achieved sufficient knockdown (>60%).

For hypertrophy studies, following transfection, the medium was replaced with fresh complete growth medium containing either 1.5 μM Angiotensin II (Ang II; MeilunBio®) or saline control. Cells were then further incubated for 36 hours to induce hypertrophic remodeling and harvested for analysis.

Table 1. Sequences of Isoform-specific siRNAs

Gene	Sequence	
	Sense(5'-3')	Antisense(5'-3')
HDAC1-Homo-988	GGUGGUUACACCAUUCGUATT	UACGAAUGGUGUAACCACCTT
HDAC2-homo-376	CCAUGAAGCCUCAUAGAAUTT	AUUCUAUGAGGCUUCAUGGTT
HDAC3-Homo-671	GCACAGGUGACAUGUAUGATT	UCAUACAUGUCACCUGUGCTT

2.3. Quantitative PCR

RNA was extracted from cultured AC16 human cardiomyocytes using the Rapid RNA Isolation Kit for Cells (Share-Bio, #SB-R001) according to the manufacturer's instructions. Complementary DNA (cDNA) was synthesized from 1 μg of total RNA using the All-in-One First-Strand Synthesis MasterMix (Share-Bio, #SB-RT001). Quantitative PCR (qPCR) was performed using the Universal SYBR Green qPCR Premix (Share-Bio, #SB-Q204) on the QuantStudio™ 5 System. See Table 2 for primer sequences. Relative gene expression was calculated using the 2^(-ΔΔCt) method.

Table 2. Sequences of qPCR Primers

Target Gene	Sequence	
	Forward	Reverse
HDAC1	CTACTACGACGGGGATGTTGG	GAGTCATGCGGATTCGGTGAG
HDAC2	ATGGCGTACAGTCAAGGAGG	TGCGGATTCTATGAGGCTTCA
HDAC3	CCTGGCATTGACCCATAGCC	CTCTTGGTGAAGCCTTGCATA
GAPDH	UGACCUCAACUACAUGGUUTT	AACCAUGUAGUUGAGGUCATT

2.4. Immunofluorescence Microscopy

AC16 human cardiomyocytes were fixed in 4% paraformaldehyde for 15 minutes at room temperature. After fixation, cells were permeabilized and blocked in a solution of 5% bovine serum albumin (BSA) and 0.1% Triton X-100 in PBS for 1 hour at room temperature. Cells were then stained with fluorescent conjugates to visualize cellular structures. F-actin was labeled using 488-Phalloidin (Share-Bio, #SB-YP0059) at a dilution of 1:100 in blocking buffer for 1 hour at room temperature. Nuclei were counterstained with DAPI included in the mounting medium. After staining, samples were washed three times with PBS and mounted using Fluoromount-G™ mounting medium. Imaging was performed using a ZEISS LSM900 laser scanning confocal microscope. Image analysis and quantification of cell surface area were performed using FIJI.

2.5. Western Blotting

Protein lysates were extracted from AC16 human cardiomyocytes using Cell Complete Lysis Buffer (Beyotime, #P0037-100ml) supplemented with protease inhibitors. Proteins were separated by gel electrophoresis and subsequently transferred to nitrocellulose membranes. Following transfer, membranes were blocked in 5% non-fat milk prepared in Tris-buffered saline with 0.1% Tween-20 (TBST) for 1 hour at room temperature. Membranes were incubated overnight at 4°C with 1:1000 diluted primary antibodies HDAC1 Rabbit Monoclonal Antibody (Beyotime, #AG8018), HDAC2 Rabbit Monoclonal Antibody (Beyotime, #AF1555), or HDAC3 Rabbit Monoclonal Antibody (Beyotime, #AF2011). The following day, membranes were washed with TBST and incubated with a 1:1000 diluted HRP-conjugated anti-rabbit secondary antibody (Cell Signaling Technology, #7074) for 1 hour at room temperature. After further washing, protein bands were visualized using FemtoDet Enhanced Chemiluminescent HRP Substrate KT (Share-Bio, #SB-WB004). Protein molecular weight was estimated using Multicolor Prestained Protein Ladder (Share-Bio, #SB-26616 and #SB-26619). Band intensity was quantified by densitometric analysis using FIJI.

3. Results

To study human cardiomyocytes *in vitro*, we chose AC16, an immortalized human cardiomyocyte line that shares basic function and structure with adult human ventricular cardiomyocytes. In this study, we focused on three isoforms of the Class I HDACs (HDAC1, 2, 3), as HDAC8 has been primarily associated with bone formation in embryonic development (Haberland et al., 2009).

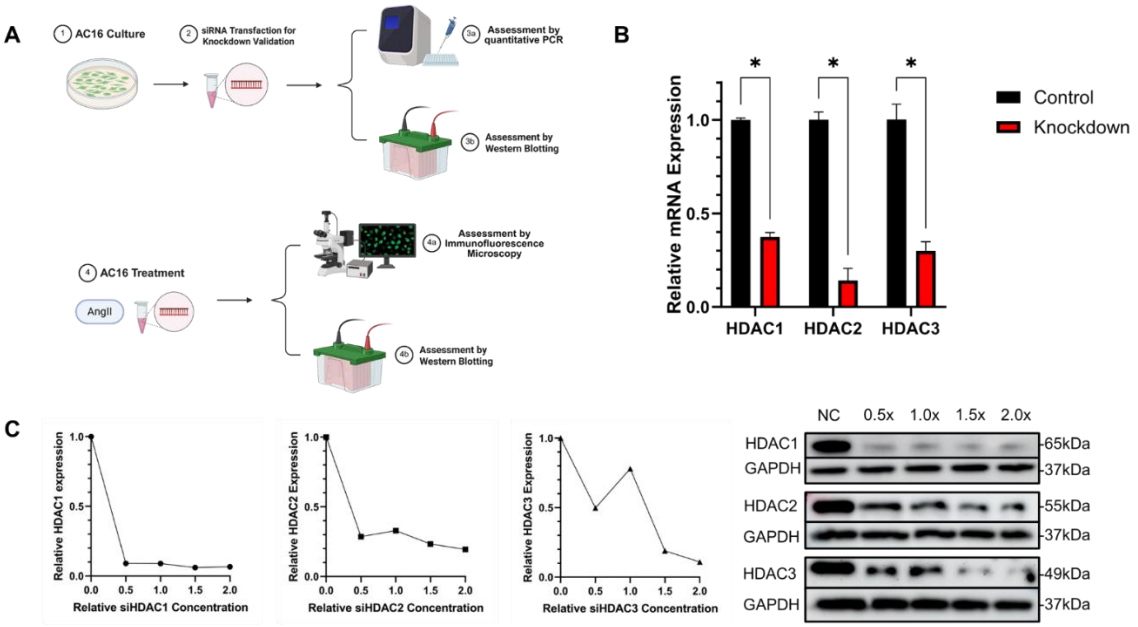

Figure 1. siRNA-mediated knockdown of Class I HDAC isoforms in AC16

(A) Schematic of the experimental timeline. AC16 cells were transfected with non-targeting (NC) or isoform-specific siRNA (siHDAC1, siHDAC2, siHDAC3). Knockdown was validated at the mRNA level by qPCR and Western Blotting at 72 hours. Validated cells were subsequently treated (NC, AngII, AngII+siHDAC1, AngII+siHDAC2, AngII+siHDAC3) and assessed for pathological remodeling progress with Immunofluorescence Microscopy and Western Blotting. (B) qPCR analysis of HDAC1, HDAC2, and HDAC3 mRNA expression 72 hours post-transfection. Data were presented as mean ± SEM. Statistical significance was determined with multiple t-tests (*$p<0.05$). (C) Representative Western blot (top) and corresponding quantitative analysis (bottom) of HDAC1, HDAC2, and HDAC3 expression levels 72 hours post-transfection with a concentration gradient of isoform-specific siRNA (0.5x, 1.0x, 1.5x, 2.0x manufacturer‘s recommended concentration) and a non-targeting siRNA (NC). GAPDH was used as a loading control. Quantification shows inhibition of HDAC expression at the 1.0x concentration (20 μM)

3.1. siRNA Knocked Down Class I HDAC Isoforms in AC16

We first employed siRNAs to knock down Class I HDAC isoforms individually (Figure 1A). AC16 human cardiomyocytes were cultured and subjected to transfection with isoform-specific siRNA targeting HDAC1, HDAC2, or HDAC3. A negative control group of AC16 was transfected with non-targeting siRNA. The efficacy of knockdown was assessed with qPCR and Western Blotting after 24 and 72 hours, respectively.

qPCR analysis validated the effective knockdown of the target HDACs (Figure 1B). In comparison to the control group, transfection with isoform-specific siRNA resulted in a significant decrease by over 60% in the relative mRNA expression for all three isoforms.

Western blot results also confirmed HDAC knockdown at the protein level (Figure 1C). The decrease in HDAC expression induced by Angiotensin II was markedly reversed across the three siRNA-treated groups. siHDAC1, siHDAC2, and siHDAC3 successfully knocked down their corresponding HDAC isoform level by over 30%. Both qPCR and western blot results demonstrated that each siRNA effectively inhibited its respective HDAC isoform expression.

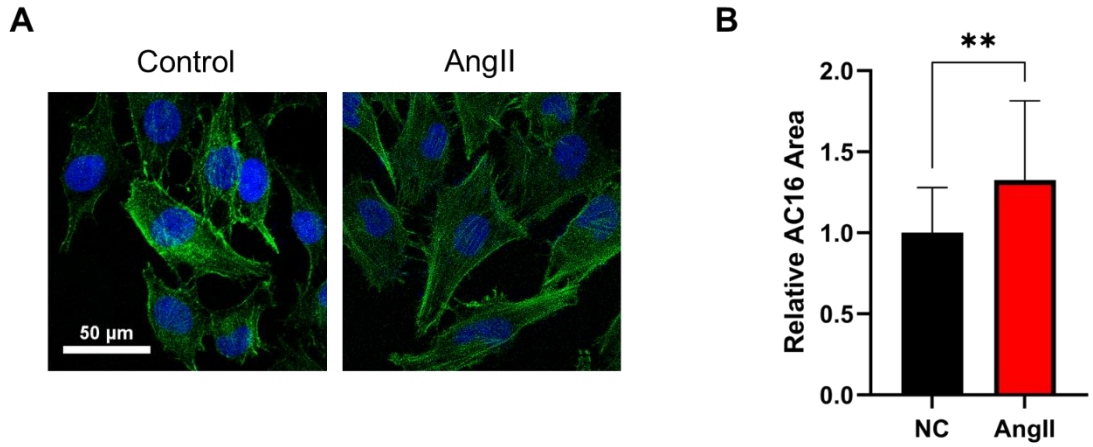

Figure 2. Angiotensin II induces hypertrophic remodeling in AC16

(A) Representative immunofluorescence images of AC16 cells showing F-actin cytoskeleton (Phalloidin-488, green) and nuclei (DAPI, blue). Cells were treated with either saline (control, left) or 1.5 μM AngII (right) for 36 hours to induce hypertrophy, resulting in a visible increase in cell surface area. Scale bar = 50 μm. (B) Quantitative analysis of cell surface area validated the hypertrophic model. AngII stimulation significantly increased the average cell area compared to the NC group. Data are presented as mean ± SEM. Statistical significance was determined with an unpaired t-test (**$p=.007$)

3.2. Angiotensin II Induced Hypertrophic Remodeling in Human Cardiomyocytes

To model pathological cardiac hypertrophy *in vitro*, we stimulated AC16 human cardiomyocytes with angiotensin II (AngII), which mimicked a hypertensive environment. This treatment induced a hypertrophic response in AC16, manifested by a significant increase in cell surface area. As shown in Figure 2A, AngII-treated cardiomyocytes were significantly larger compared to the control group. Quantitative analysis of the AC16 surface area revealed that AngII stimulation increased the average cell area by 31.96%, confirming the establishment of the hypertrophic model.

The pathological remodeling was further confirmed by evaluating the expression of beta-myosin heavy chain (β-MHC/MYH7), a canonical biomarker of pathological hypertrophy. Western blot analysis demonstrated a significant upregulation of MYH7 in response to AngII (Figure 2B). The relative MYH7 expression level increased by 53.37% on average in the AngII-treated group compared to the control, validating the hypertrophic model.

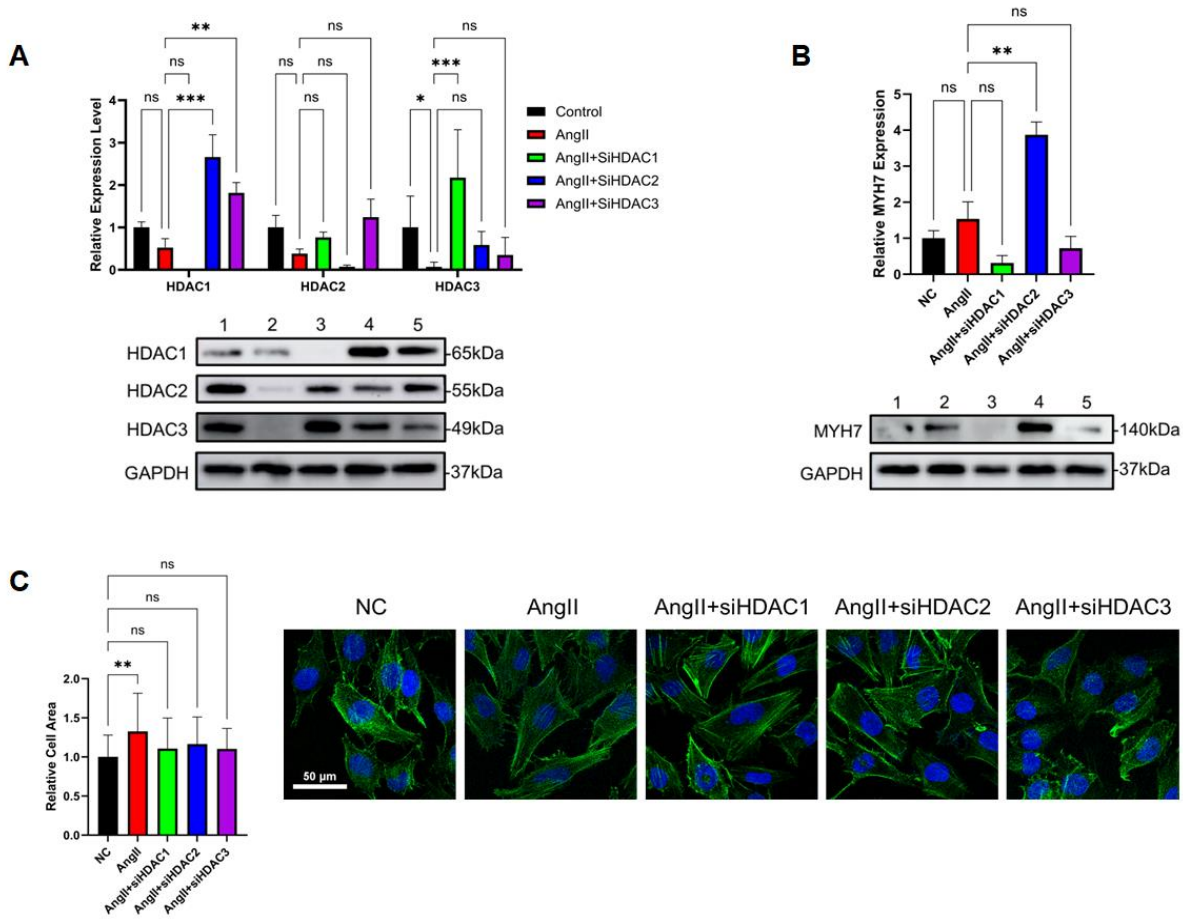

Figure 3. Class I HDAC isoforms exhibit differential roles in cardiac hypertrophy

(a) Quantitative analysis of HDAC1, HDAC2, and HDAC3 protein expression after siRNA transfection and AngII treatment. For each target HDAC on the x-axis, the five treatment groups (NC, AngII, AngII+siHDAC1, AngII+siHDAC2, AngII+siHDAC3) showed the relative expression level of that specific isoform. Data were presented as mean relative expression ± SEM. Statistical significance was determined with two-way ANOVA (***p<.001; **p=.004; *p=.043). (B) Representative Western blot (bottom) and quantitative analysis (top) of MYH7. AngII stimulation significantly increased MYH7 expression. Silencing of HDAC1 or HDAC3 reversed the AngII-induced MYH7 upregulation, whereas HDAC2 knockdown reinforced it. Data were presented as mean relative expression ± SEM. Statistical significance was determined with one-way ANOVA (AngII vs. AngII+siHDAC2, **p=.004). (C) Representative immunofluorescence images (right) and quantitative analysis of cell surface area (left) of the five treatment groups (NC, AngII, AngII+siHDAC1, AngII+siHDAC2, AngII+siHDAC3) stained for F-actin (Phalloidin-488, green)

and nuclei (DAPI, blue). Scale bar = 50 μm. AngII treatment increased cell area. Knockdown of HDAC1, HDAC2, or HDAC3 all reversed the AngII-induced cellular enlargement. Data are presented as mean relative cell area ± SEM. Statistical significance was determined with one-way ANOVA (NC vs. AngII, **p=.008).

3.3. Class I HDAC Isoforms Mediate Differential Responses to Hypertrophic Stimulation

Pathological stimulation with AngII significantly altered the expression profiles of the Class I HDAC isoforms (Figure 3A). Surprisingly, western blot results exhibited that AngII treatment alone downregulated all three isoforms by over 40% compared to the control group, which is speculated to be a compensatory mechanism against the cell stress. In addition, all isoform-specific siRNAs maintained the silencing effects in the presence of AngII. Interestingly, while Western Blotting for the Class I HDACs confirmed the efficacy and specificity of each siRNA, a complex pattern of cross-isoform interference was also revealed. HDAC1 knockdown suppressed the HDAC2 level (to 76.5% of control), while potently increasing HDAC3 expression (to 217.5% of control); HDAC2 knockdown suppressed the HDAC3 level (to 58.5% of control), while potently increasing HDAC1 expression (to 266.0% of control). siHDAC3 resulted in upregulation of both HDAC1 and HDAC2, with an increase of 81.4% and 23.9%, respectively.

The influence of isoform-specific HDAC inhibition on hypertrophic remodeling was assessed by measuring MYH7 expression (Figure 3B). The AngII stimulation alone induced a significant increase in MYH7 levels, 53.37% from control. The knockdown of individual HDAC isoforms in the hypertrophy model produced divergent effects on MYH7 expression. The silencing of HDAC1 and HDAC3 suppressed MYH7 expression, reducing it to 31.4% and 72.1% of the control level, respectively. In contrast, HDAC2 knockdown surprisingly exacerbated the hypertrophic response, resulting in a profound upregulation of MYH7 to 315.3% of control.

The distinct influence of HDAC isoform inhibition was further investigated by morphological analysis of AC16. As shown in Figure 3C, AngII stimulation induced cellular enlargement, increasing the average cell area to 132.0% of the control group. All HDAC knockdown groups exhibited different hypertrophy-reversing effects, as shown by decreased surface areas. HDAC1 and HDAC3 knockdown displayed similar beneficial effects, evidenced by only 10% increase in the cell area. This result was aligned with the previous downregulated MYH7 result. The HDAC2 knockdown group had a cell area of 116.4% of control, demonstrating a reverse effect to remodeling, which contrasts with its exacerbating effect at the protein level.

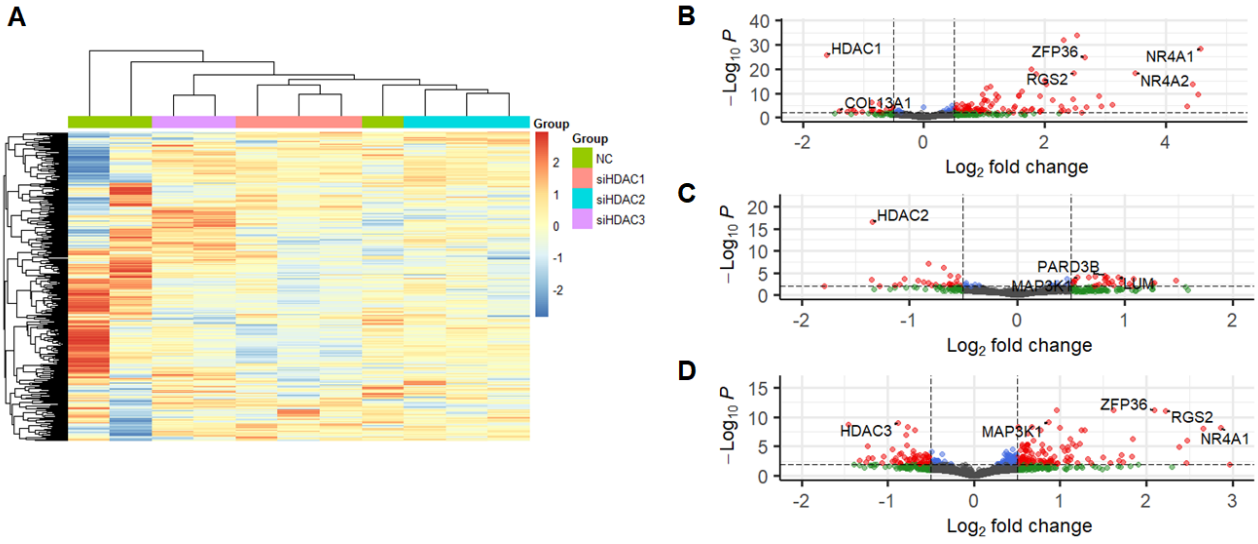

Figure 4. RNA sequencing reveals distinct transcriptomic profiles driven by individual HDAC knockdown in a hypertrophic model

(A) Heatmap of global gene expression profiles for AngII-treated AC16 cells transfected with non-targeting (NC) or isoform-specific siRNA (siHDAC1, siHDAC2, siHDAC3). Each column represents

an individual sample. (B-D) Volcano plots of differentially expressed genes (DEGs) for (B) siHDAC1 vs. NC, (C) siHDAC2 vs. NC, and (D) siHDAC3 vs. NC comparisons. Key annotated genes have known functions in cardioprotection or pathological remodeling.

3.4. RNA Sequencing Revealed Distinct Gene Expression Profiles in Individual siHDAC-treated Hypertrophy

To obtain a deeper understanding of how individual HDACs regulate hypertrophic signaling, we performed bulk RNA sequencing analysis for cells treated with AngII together with either control siRNA (NC) or individual siHDACs.

The heatmap demonstrated that global gene expressions in the control group were distinctly different from those of other siHDAC-treated cells (Figure 4A). Moreover, the three siHDAC groups differed from one another, exhibiting distinct patterns of gene upregulation and downregulation. To investigate which top differentially expressed genes (DEGs) were involved, we generated volcano plots for comparisons between siHDAC1 and NC, siHDAC2 and NC, and siHDAC3 and NC.

Consistent with previous results, siHDAC1 treatment upregulated multiple genes that were reported to be protective against hypertrophy (Figure 4B). For example, *NR4A1* and *NR4A2* are known to inhibit stress responses such as isoproterenol-mediated hypertrophy (Yan et al., 2015). *RGS2* is a regulator downregulating GPCR signaling, which promotes pathological cardiac hypertrophy (Chidiac et al., 2014). *ZFP36* plays a protective role in suppressing mTORc1 activity, which is crucial in cardiac remodeling (Kouzu et al., 2022). In the downregulated DEGs, we found *COL13A1*, a gene encoding fibrosis-associated proteins.

The DEGs identified in siHDAC2-treated cells were distinct from those observed in siHDAC1-treated cells (Figure 4C). In the upregulated DEGs, *MAP3K1* plays a potentially protective role in cardiomyocyte survival and inflammation reduction under pressure overload (Suddason & Gallagher, 2015). However, *PARD3* and *LUM* were two DEGs that were found to promote pathological hypertrophy, which may explain why MYH7 was elevated by siHDAC2 in our previous result (Dupuis et al., 2015).

siHDAC3-treatment also showed an anti-hypertrophy profile (Figure 4D). Similar to DEGs identified in the siHDAC1 group, *NR4A1*, *ZFP36*, *MAP3K1*, and *RGS2* were upregulated, which indicated cardioprotection against hypertrophic remodeling.

3.5. Differential Regulation of Class I HDACs in Patient Left Ventricles

To relate our findings to clinics, we analyzed RNA-seq of hypertrophic left ventricles collected from patients who had hypertrophic cardiomyopathy (HCM) or aortic stenosis (AS). The sequencing data were obtained from a previously published dataset (Burkart et al., 2023). As shown in Figure 5, compared to the healthy group, cardiac tissues from both HCM and AS diseases had significantly decreased HDAC1 expression. This aligns with our findings that HDAC1 may be a critical factor regulating hypertrophic remodeling. Interestingly, HDAC2 was significantly increased in the diseased tissues, suggesting its compensatory and beneficial function, as we previously demonstrated. HDAC3 remained unchanged in both disease conditions.

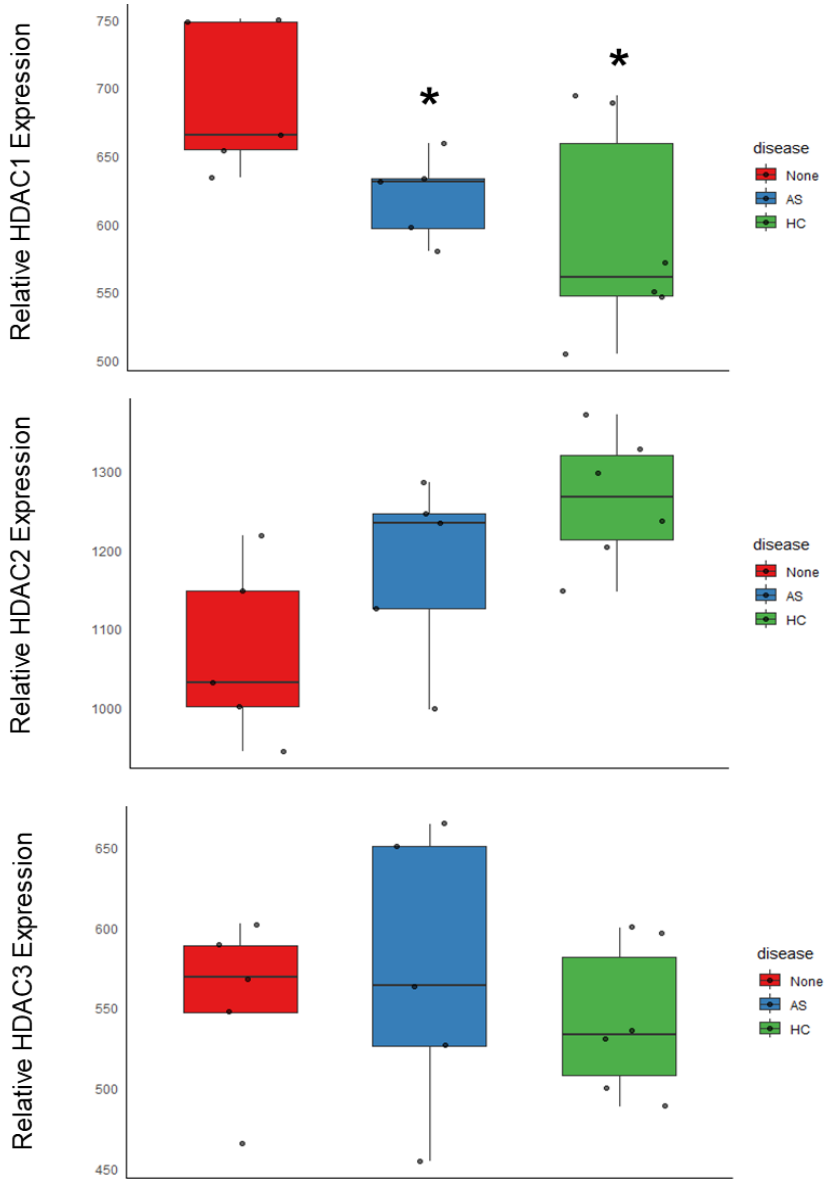

Figure 5. Differential mRNA expression of Class I HDACs in human hypertrophic cardiomyopathy

Relative mRNA expression levels (normalized counts) of HDAC1, HDAC2, and HDAC3 in left ventricular tissue from healthy donors and patients with hypertrophic cardiomyopathy (HCM) or aortic stenosis (AS). Data are from a publicly available dataset (Burkart et al., 2023). HDAC1 was significantly downregulated in disease, HDAC2 was significantly upregulated, and HDAC3 remained unchanged (*p<.001).

4. Discussion

This study provided new insights into the involvement of individual Class I HDAC isoforms in cardiac pathological hypertrophy induced by angiotensin II. In the past decade, HDACs have been believed to be associated with hypertrophy. Previous studies demonstrated that pressure-overload hypertrophy could be significantly attenuated with the treatment of pan-HDAC inhibitors *in vivo* and *in vitro*. Later studies further delineated the effects of HDAC and confirmed Class I HDAC as a potential group of therapy targets for heart failure. However, the application of HDAC inhibitors to hypertrophic patients has been facing challenges, because patients in clinical trials developed drug resistance and, more importantly, current FDA-approved drugs are repurposed from cancer therapy, which do not have ideal specificity to a certain class and therefore do not meet cardiac therapy demand.

Although siRNAs have also been used to inactivate the Class I HDACs and show cardioprotection, we still have a limited understanding of each isoform to decide which HDACs need to be silenced.

The most notable result of our work is the significant functional divergence of the Class I HDACs. Across the isoforms investigated, inhibition of HDAC1 and HDAC3 was effective in reversing cardiac hypertrophy by successfully repressing expression of *MYH7* and reducing cell surface area, whereas inhibiting HDAC2 produced an opposing response. This finding directly challenges previous treatment schemes in which people presumed the Class I HDACs had a consistent tendency to blunt hypertrophic signaling. Furthermore, our results suggested that HDAC2 has a distinctly different role in cardiac hypertrophy. Indiscriminate inhibition of all Class I HDACs, which may offset its advantages by concurrently inhibiting beneficial isoforms (HDAC2) or losing focus in suppressing the most harmful isoforms (HDAC1 and 3). Therefore, a highly selective HDAC inhibitor may be promising to provide more precise treatment for cardiac hypertrophy.

What is exciting is that we found similar trends in patients' hypertrophic cardiac tissues. In patients with HCM or AS, the expression of HDAC1 was downregulated, whereas HDAC2 was increased. The finding enhanced our explanation that HDAC2 may be involved in a protective mechanism to compensate for hypertrophy-associated dysfunction. Further investigations may be undertaken to examine the expression levels of Class I HDACs in other cardiac diseases, such as dilated cardiomyopathy and ischemic cardiomyopathy.

In summary, our determination of isoform-specific distinctions in the Class I HDACs offers a compelling knowledge foundation from which to launch future research in other HDAC classes or pharmaceutical developments with better specificity. We also speculated that such functional variations may exist among Class II HDACs, which have been previously defined as repressors of cardiac hypertrophy. An individualized, isoform-specific approach similar to that used herein for each member of Class II HDACs may be essential to a detailed investigation of their exact roles in cardiac pathology. Such work will prove crucial in the comprehensive determination of HDAC's role in cardiac pathology, available as a foundation upon which to develop future epigenetic therapies.

References

[1] Burkart, V., Kowalski, K., Disch, A., Hilfiker-Kleiner, D., Lal, S., Remedios, C. dos, Perrot, A., Zeug, A., Evgeni Ponimaskin, Kosanke, M., Dittrich-Breiholz, O., Kraft, T., & Montag, J. (2023). Nonsense mediated decay factor UPF3B is associated with cMyBP-C haploinsufficiency in hypertrophic cardiomyopathy patients. *Journal of Molecular and Cellular Cardiology*, *185*, 26–37. https://doi.org/10.1016/j.yjmcc.2023.09.008

[2] Chidiac, P., Sobiesiak, A. J., Lee, K. N., Gros, R., & Nguyen, C. H. (2014). The eIF2B-interacting domain of RGS2 protects against GPCR agonist-induced hypertrophy in neonatal rat cardiomyocytes. *Cellular Signalling*, *26*(6), 1226–1234. https://doi.org/10.1016/j.cellsig.2014.02.006

[3] Dupuis, L. E., Berger, M. G., Feldman, S., Doucette, L., Fowlkes, V., Chakravarti, S., Thibaudeau, S., Alcala, N. E., Bradshaw, A. D., & Kern, C. B. (2015). Lumican deficiency results in cardiomyocyte hypertrophy with altered collagen assembly. *Journal of Molecular and Cellular Cardiology*, *84*, 70–80. https://doi.org/10.1016/j.yjmcc.2015.04.007

[4] Gillette, T. G. (2021). HDAC Inhibition in the Heart: Erasing Hidden Fibrosis. *Circulation*, *143*(19), 1891–1893.

[5] Gillette, T. G., & Hill, J. A. (2015). Readers, Writers, and Erasers. *Circulation Research*, *116*(7), 1245–1253. https://doi.org/10.1161/circresaha.116.303630

[6] Haberland, M., Mokalled, M. H., Montgomery, R. L., & Olson, E. N. (2009). Epigenetic control of skull morphogenesis by histone deacetylase 8. *Genes & Development*, *23*(14), 1625–1630. https://doi.org/10.1101/gad.1809209

[7] Kee, H. J., Sohn, I. S., Nam, K. I., Park, J. E., Qian, Y. R., Yin, Z., Ahn, Y., Jeong, M. H., Bang, Y.-J., Kim, N., Kim, J.-K., Kim, K. K., Epstein, J. A., & Kook, H. (2006). Inhibition of Histone Deacetylation Blocks Cardiac Hypertrophy Induced by Angiotensin II Infusion and Aortic Banding. *Circulation*, *113*(1), 51–59. https://doi.org/10.1161/circulationaha.105.559724

[8] Kong, Y., Tannous, P., Lu, G., Berenji, K., Rothermel, B. A., Olson, E. N., & Hill, J. A. (2006). Suppression of Class I and II Histone Deacetylases Blunts Pressure-Overload Cardiac Hypertrophy. *Circulation*, *113*(22), 2579–2588. https://doi.org/10.1161/circulationaha.106.625467

[9] Kouzu, H., Tatekoshi, Y., Chang, H.-C., Shapiro, J. S., McGee, W. A., Jesus, A. D., Ben-Sahra, I., Arany, Z., Leor, J., Chen, C., Blackshear, P. J., & Ardehali, H. (2022). ZFP36L2 suppresses mTORc1 through a P53-dependent pathway to prevent peripartum cardiomyopathy in mice. *Journal of Clinical Investigation*, *132*(10). https://doi.org/10.1172/jci154491

[10] Morales, C. R., Li, D. L., Pedrozo, Z., May, H. I., Jiang, N., Kyrychenko, V., Cho, G. W., Kim, S. Y., Wang, Z. V., Rotter, D., Rothermel, B. A., Schneider, J. W., Lavandero, S., Gillette, T. G., & Hill, J. A. (2016). Inhibition of class I histone deacetylases blunt cardiac hypertrophy through TSC2-dependent mTOR repression. *Science Signaling*, *9*(422). https://doi.org/10.1126/scisignal.aad5736

[11] National Center for Cardiovascular Diseases, The Writing Committee of the Report on Cardiovascular Health and Diseases in China. (2024). Report on Cardiovascular Health and Diseases in China 2023: An Updated Summary. *PubMed*, *37*(9), 949–992. https://doi.org/10.3967/bes2024.162

[12] Suddason, T., & Gallagher, E. (2015). A RING to rule them all? Insights into the Map3k1 PHD motif provide a new mechanistic understanding into the diverse roles of Map3k1. *Cell Death & Differentiation*, *22*(4), 540–548. https://doi.org/10.1038/cdd.2014.239

[13] Yan, G., Zhu, N., Huang, S., Yi, B., Shang, X., Chen, M., Wang, N., Zhang, G., Talarico, J. A., Tilley, D. G., Gao, E., & Sun, J. (2015). Orphan Nuclear Receptor Nur77 Inhibits Cardiac Hypertrophic Response to Beta-Adrenergic Stimulation. *Molecular and Cellular Biology*, *35*(19), 3312–3323. https://doi.org/10.1128/mcb.00229-15